Master Advanced Lab Course
Universität Göttingen – Fakultät für Physik

Report on the experiment FM.ULP

Spatial and Temporal Distortions of Ultrashort Light Pulses

Name:	Kieran Amos
Email:	kieranrobert.amos@stud.uni-goettingen.de
Conducted on	22nd November 2017
Assistant:	Dr. Sabine Steil
Copy of document requested:	☐ yes ☑ no
Unterschrift:	

Submission

Date: Signature of assistant:

Review

Date: Name of examiner:

Points: Signature:

Mark:

Contents

1 Introduction **1**

2 Theory **2**
2.1 Ultrafast Laser Pulses 2
2.2 Temporal Chirp 3
2.3 Spatial Chirp and Pulse-Front Tilt 3
2.4 Prism Compressor 4

3 Experimental Setup **5**

4 Results **7**
4.1 Adjusting the Prism Compressor 7
4.2 Optical Windows 7
4.3 The Second Bandwidth 9

5 Discussion **9**

1 Introduction

In recent years, the field of optics has seen the development of lasers capable of generating ultrafast electromagnetic pulses. These high-intensity pulses occur on a time scale of femtoseconds (10^{-15} s) or less and can thus be used to probe physical processes that occur over a similar duration. The technique has had considerable success in femtochemistry, where chemical processes can be characterised that are otherwise be inscrutable to conventional methods. Other applications currently in development include advanced material processing at the sub-micrometer scale and micro-machining.
A common form of ultrafast pulses is a chirped Gaussian, where the amplitude of the electromagnetic field is enveloped by a gaussian function and the instantaneous frequency varies over the course of the pulse.
In order to take full advantage of this method, it is necessary to understand the mechanisms responsible for introducing spatial and temporal distortions to the beam pulse and how these distortions be compensated.
In this experiment the frequency and temporal range of a chirped gaussian pulse is evaluated using a pulse characterisation device utilising the GRENOUILLE method, capable of measuring the pulse-front tilt and spatial chirp. Different optical elements are inserted into the beam path and their effects on the beam are observed and then mitigated using a prism compressor.
The observations are then compared with the expected outcomes based off theoretical calculations as well as the results obtained from a simulation of the same setup using the computer software VCHIRP.

2 Theory

2.1 Ultrafast Laser Pulses

The propagation of electromagnetic waves is described via the wave equation with the solution being plane waves of the form

$$\vec{E}(\vec{r},t) = \vec{E}_0 \exp\Big[i(\omega_0 \cdot t - \vec{k}\cdot\vec{r} + \phi_0)\Big], \tag{2.1}$$

where $\vec{E}_0$ is the initial amplitude, ω_0 is the wave frequency and $\vec{k}$ the wave vector. ϕ_0 denotes the phase factor at $t = 0$.
Superimposing multiple plane waves of varying frequencies leads to wave packages that are temporally localised and are often of a gaussian form. Ignoring the spatial component and simplifying to one dimension, one can describe envelope function of the wave package as follows:

$$E(t) = A(t)\exp\left[i\phi(t)\right]. \tag{2.2}$$

The rapidly oscillating phase within the enveloping function has here been neglected and the pulse is completely described by a real amplitude $A(t) = \sqrt{I(t)}$ with $I(t)$ the intensity and a phase, $\phi(t)$.
This equation can be expressed in the frequency domain via a Fourier transformation:

$$\tilde{E}(\omega) = \frac{1}{\sqrt{2\pi}}\int_{-\infty}^{\infty} E(t)e^{-i\omega t}\mathrm{d}t = \tilde{A}(\omega)\exp\left[i\varphi(\omega)\right]. \tag{2.3}$$

When propagating through a medium, a phase is added, that is proportional to the refraction index, n, of the material and the distance traversed, d:

$$\varphi(\omega) = k(\omega)\cdot d\cdot n(\omega). \tag{2.4}$$

The phase can also be expressed in dependence on the wavelength, λ with $\omega(\lambda) = \frac{2\pi c}{\lambda}$ and c the speed of light in a vacuum. The wave vector is given by $k(\lambda) = \frac{2\pi}{\lambda}$.
The refraction index of a material is in general wavelength dependent. The dependence can be described empirically via the Sellmeier equation with the Sellmeier coefficients $B_{1,2,3}$, and $C_{1,2,3}$ determined experimentally for each material:

$$n(\lambda) = \sqrt{\frac{B_1\lambda^2}{\lambda^2 - C_1} + \frac{B_2\lambda^2}{\lambda^2 - C_2} + \frac{B_3\lambda^2}{\lambda^2 - C_3} + 1}. \tag{2.5}$$

If the phase is Taylor expanded around the carrier frequency, the first few terms are usually sufficient to describe the properties of the ultrafast pulse:

$$\varphi(\omega) = \varphi_0 + \varphi_1\frac{\omega - \omega_0}{1!} + \varphi_2\frac{(\omega-\omega_0)^2}{2!} + ... \tag{2.6}$$

The first term is constant and has no effect on the shape of the pulse. The second, linear term also does not influence the shape but leads via the Fourier Transform Shift Theorem to a shift of the total pulse along the time axis and is hence called the Group Delay (GD):

$$GD = \left.\frac{d\varphi}{d\omega}\right|_{\omega_0}. \tag{2.7}$$

Of most interest to this experiment is the second order term, referred to as the Group Delay Dispersion (GDD). The effect is to impart different group velocities to the different frequencies and thus broaden an initially compact pulse with either higher or lower frequencies arriving first depending on the sign of the GDD. The presence of GDD is often referred to as temporal chirp due to the sound perceived when the pulse is converted to audio.

$$GDD = \left.\frac{d^2\varphi}{d\omega^2}\right|_{\omega_0}. \tag{2.8}$$

The width of a gaussian pulse is typically described by the full width of the enveloping function at half its maximum (FWHM). Assuming an initially unchirped pulse of width $\tau_{FWHM,0}$, one can relate the final width τ_{FWHM} to the GDD via the following equation:

$$\tau_{FWHM} = \sqrt{\tau_{FWHM,0}^2 + \left(2\ln(2)\cdot GDD\cdot\Delta\omega\right)^2}, \tag{2.9}$$

where $\Delta\omega$ is the frequency bandwidth of the initial pulse, $\Delta\omega = \frac{2\pi c\Delta\lambda}{\lambda^2}$.

2.2 Temporal Chirp

Combining Equations 2.4 and 2.8 it is apparent that temporal chirp occurs when the refraction index of a material, n has a non vanishing derivative with regard to the wavelength, $\frac{d^2n}{d\lambda^2} > 0$. The formula used to determine the GDD gained when the beam propagates through a dispersive medium is

$$GDD = \frac{\lambda^3}{4\pi c^2}\frac{d^2n}{d\lambda^2}L_g, \tag{2.10}$$

where L_g is the path length of the carrier frequency through the glass.
In the case where the beam hits the glass at an angle, the formula needs to accommodate the extra path length due to refraction according to Snell's law. With α the angle of incidence and β the angle of refraction within the medium, Snell's law gives

$$\beta = \arcsin\frac{\sin\alpha}{n}, \tag{2.11}$$

with $n = n_{glas}$ and $n_{air} \approx 1$. The abth length within meanwhile is increased by

$$L_g = \frac{d}{\cos\beta}, \tag{2.12}$$

where d is the width of the window. Combining the two leads to the following modification of Equation 2.10:

$$GDD = \frac{\lambda^3}{4\pi c^2}\frac{d^2n}{d\lambda^2}\frac{d}{\cos\left(\arcsin\frac{\sin\alpha}{n}\right)} = \frac{\lambda^3}{4\pi c^2}\frac{d^2n}{d\lambda^2}\frac{d}{\sqrt{1-\frac{\sin^2\alpha}{n^2}}}. \tag{2.13}$$

2.3 Spatial Chirp and Pulse-Front Tilt

Spatial chirp occurs when different wave lengths are spatially displaced at right angles to the beam direction. This occurs when the beam does not hit an optical element perpendicularly and the transmitted angle varies across the spectrum according to Snell's law. The wavelengths will then exit the optical element at different locations and the beam will be spread out spatially with higher frequencies bunching to one side of the pulse and lower frequencies at the other as shown in Figure 1. The same effect occurs when the beam traverses a single prism.
Pulse-front tilt on the other hand is characterised by a tilt of the pulse in the direction of propagation. It can be seen

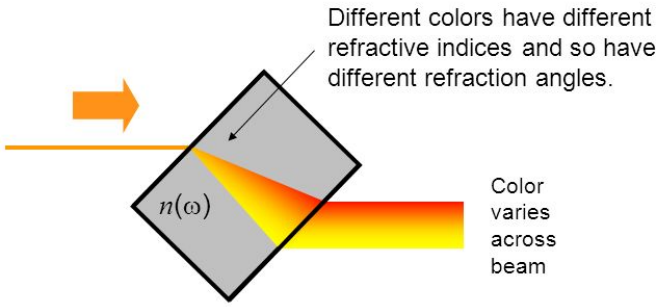

Figure 1: Illustration of spatial chirp when an unchirped pulse transverses a tilted optical window.

as the combined effects of temporal and spatial chirp and is of primary concern for an ill-adjusted prism compressor, or if a pulse has previously acquired a spatial chirp before entering an optical element as in Figure 2. The varying flight times of the wavelengths will tilt the pulse with faster photons exiting the material ahead of the slower ones.

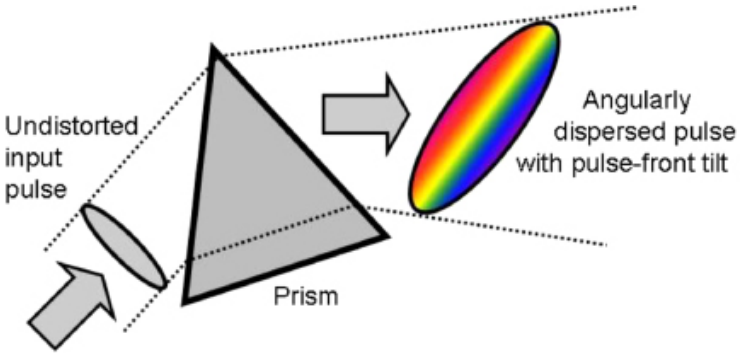

Figure 2: Example of introduction of pulse-front tilt when a spatially chirped pulse encounters a dispersive medium.

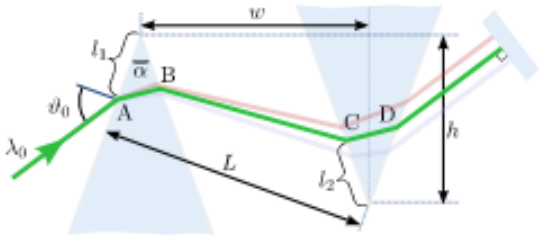

Figure 3: Basic setup of a prism compressor.

2.4 Prism Compressor

Prism compressors are often used to introduce negative GDD and in this experiment one is used to compensate for the second order dispersion of various optical elements. The layout is shown in Figure 3. The first prism splits the beam according to the wavelengths involved and imparts each with different angle of refraction,resulting in different path lengths. The second prism causes the rays to be parallel once more and upon reflection and repeat propagation through both prisms, the beams leave the compressor with no spatial propagation. Adjusting the insertion, l_2 of the second prism varies the path length in the medium, L_g, of the carrier frequency and thus allows for different amounts of second order dispersion to be introduced.
The equation used to obtain the dispersion is as follows:

$$GDD = \frac{2\lambda_0^3}{2\pi c^2}\left[L_g \frac{d^2n}{d\lambda^2}\bigg|_{\lambda_0} - (4L + \frac{L_g}{n(\lambda_0)^3}\left(\frac{dn}{d\lambda}\bigg|_{\lambda_0}\right)^2\right]. \tag{2.14}$$

λ_0 is the wavelength of the carrier frequency and L is the separation between the two prism apexes. The functional form of the refraction index, n, and its wavelength derivatives can be obtained from Equation 2.5.
The dependence of L_g on the insertion is as follows:

$$L_g = \frac{2l_2}{\sqrt{1 + n(\lambda_0)^2}}. \tag{2.15}$$

This leads to an expected linear dependence between insertion and resulting GDD. The insertion of the first prism is assumed to be minimal, $l_1 \approx 0$. It should be noted that the prism compressors also introduce small levels of higher order dispersions but these are not discussed here.

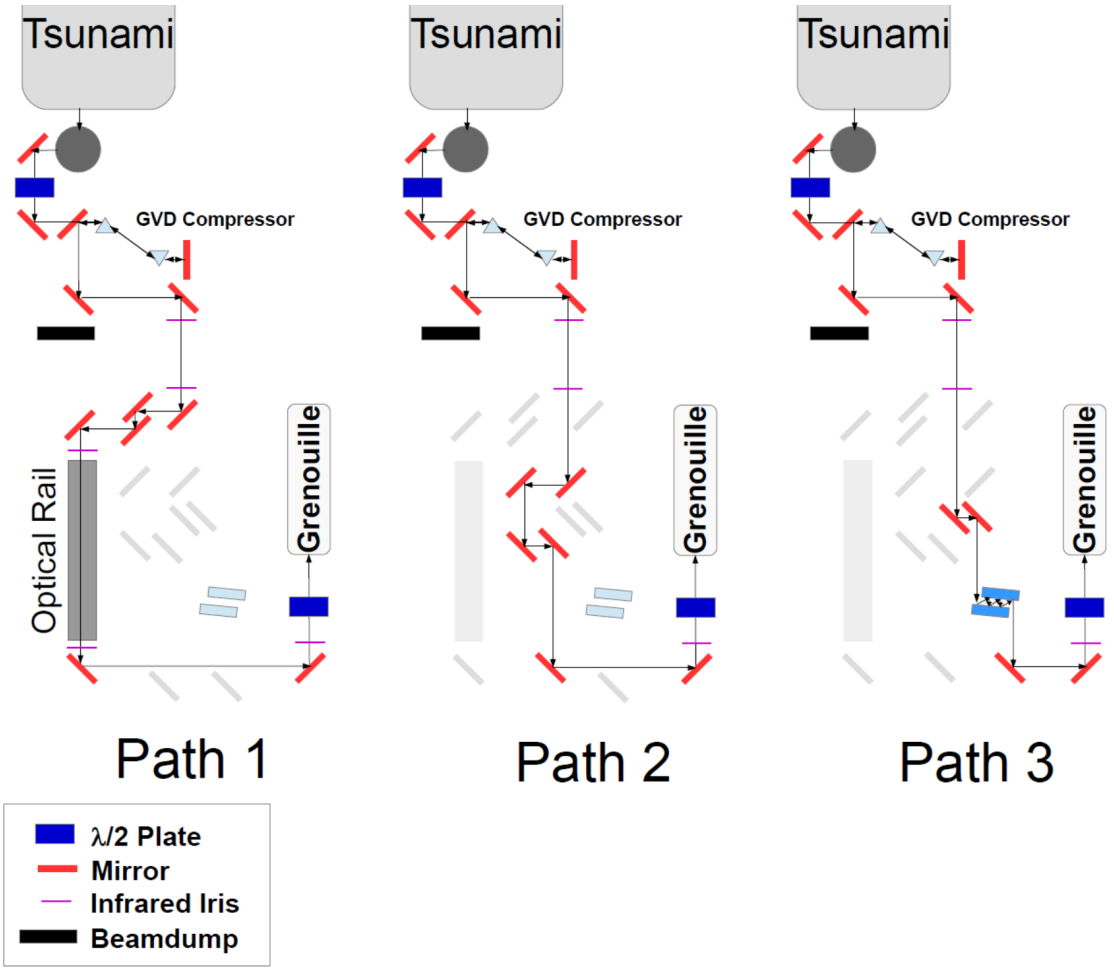

Figure 4: The three configurations for the beam path in the experiment.

3 Experimental Setup

The source of the femtosecond pulses in this experiment is a laser by Tsunami, operating at a wavelength of 800 nm with an averaged power of approximately 400 mW. The pulse length and bandwidth can be varied and for the first portion of the experiment were set to 25 fs and 55 nm respectively. The characterisation of the pulse is done using a GRENOUILLE device by Swamp Optics connected to a computer with the associated software installed. Two $\lambda/2$ plates, one directly after the laser, and the in front of the GRENOUILLE device allow for the control of the beams intensity as it reaches the readout. A prism compressor with the second prism adjustable vie a micrometer screw allows for the adjustment of the second order dispersion. After the compressor, three different beam paths to the Swamp Optics apparatus are possible depending on the configuration of dielectric mirrors. The possible layouts are displayed in Figure 4. The infrared irises are used only for the initial adjustment of the beam.
For the first part of the experiment with beam path 1, no elements are on the optical rail and measurements are taken for various insertions of the second prism. In particular the optimal setting for the minimisation of the GDD as determined by the measured pulse suration at FWHM is noted.
Next various optical elements are introduced to the optical rail at the optimal setting of the compressor and their effects on the beam are measured. In each case the prism is compressor is subsequently adjusted in an attempt to mitigate the observed effects, with the pulse duration at FWHM being the deciding criterion.
This is done for the following elements:

- One and two 5 mm of BK7 window.
- 5 mm of MgF2 window.

- 5 mm of BK7 window. tilted at an angle of $\pm 30°$.
- A MgF2 wedge with an angle of $6°$.
- A longpass filter.

The procedure is then repeated for beam path 2 which features silver mirrors instead of dielectric ones and for beam path 3 where the beam is reflected multiple times between a set of square mirrors.
Finally the bandwidth of the laser is adjusted to 27 nm and beam path 1 is repeated for the initial prism compressor setup as well as the the two BK7 windows.

4 Results

4.1 Adjusting the Prism Compressor

For the initial adjustment of the prism compressor the distance between the two prism apexes was first measured to be $L = 432 \pm 3\,\text{mm}$. To relate the insertion of the second prism to the scale displayed on the micrometer screw, the prism was adjusted until the laser beam just bypassed the apex and the position on the micrometer screw was noted. The difference between this value and any subsequent measurements was then assumed to be the insertion. To determine the properties of the unchirped pulse, the insertion was next adjusted until the pulse duration was minimised as reported by the software controlling the GRENOUILLE characterisation device. This was found to be the case for an insertion of $l_2 = 2.84\,\text{mm}$ henceforth referred to as the optimum prism insertion, where the laser consequently had a carrier frequency of $\lambda_0 = 790\,\text{nm}$, a pulse duration of $\tau_{FWHM,0} = 24.5\,\text{fs}$ and a wave-length bandwidth of $\Delta\lambda = 46.3\,\text{nm}$, corresponding to a frequency bandwidth of $\Delta\omega = 14.0\,\text{fs}^{-1}$ according to the equation

$$\Delta\omega = \frac{2\pi c \Delta\lambda}{\lambda^2}. \tag{4.1}$$

In the following step, the prism insertion was varied over approximately $3\,\text{mm}$ and the resulting pulse widths were recorded.
To calculate the GDD induced by a given insertion, Equation 2.15 was inserted into Equation 2.14 along with the expression for the refraction index, Equation 2.5, and its derivatives. The Sellmeier coefficients for the N-LAK21 prism pair were taken from.
Error propagation was calculated based of an initial error of $\sigma_L = 3\,\text{mm}$, $\sigma_{l_2} = 0.1\,\text{mm}$ and $\sigma_{\Delta\lambda} = 1\,\text{nm}$ for the respective quantities.
Since the prism configuration at optimum insertion is assumed to lead to an unchirped pulse, the associated GDD value is subtracted from the other values. The result is then the dispersion believed to contribute to the temporal broadening of the pulse.
Finally the expected pulse duration was calculated from this GDD using Equation 2.9 where error propagation was once again used with $\sigma_{\tau_{FWHM,0}} = 1\,\text{fs}$. The resulting expected pulse duration, along with the actual measurements can be seen in Figure 4.1. Equation 2.9 has been linearised by plotting the square of the pulse duration, τ_{FWHM} over the square of the GDD. This allows for easier analysis of any discrepancies. The minute errors on the measured pulse duration are obtained by observing the fluctuations as reported for the first and last measurement points by the software and linearly interpolating the rest.

The data is in good agreement with the theory, with the statistical errors accounting for all but the last two data points. These two measurements were taken at the very edge of the second prism apex, where it is likely that part of the beam was no longer hitting the prism, thus skewing the results.

4.2 Optical Windows

Both one and two $5\,\text{mm}$ BK7 optical windows were placed in the beams path, while the prism compressor was in the optimum position. Their effects were observed and an attempt was made to mitigate said effects by varying the prism insertion until the pulse duration was the same as it was without without the optical element. The GDD induced at this insertion, once again calculated according to Equation 2.14 was compared to the expected GDD gain from the BK7 glass as predicted by Equation 2.10 with the Sellmeier coefficients taken from.
The dispersion is expected to be linearly dependent on the path length, L_g, and this is indeed observed to be the case for the compensated GDD. The absolute of the GDD is plotted against $0\,\text{mm}$, $5\,\text{mm}$ and $10\,\text{mm}$ of BK7 glass both for the theoretical prediction and the required compensation in Figure 4.2. The numerical results are displayed in Table 1. Also shown are the results for the $5\,\text{mm}$ MgF2 glass and the BK7 glass tilted at a $\pm 30^\circ$ angle. In the latter case, the adjusted path length due to the internal refraction of the beam was accounted for, by utilising Equation 2.13 instead of 2.10. the statistical errors on the quantities involved in the theoretical calculation are assumed to be negligible.
The data shows an astonishing agreement for the single BK7 glass and only a discrepancy of about 5% for the double window. In the case of the MgF2 however, the theory and experiment differ by a whole magnitude. Our measurements show that the addition of the glass did not increase the pulse duration as expected. This is probably due to mismanagement of the data, or to it being captured at the wrong time. It is also possible that the beam failed to hit the glass entirely, although we think this unlikely.

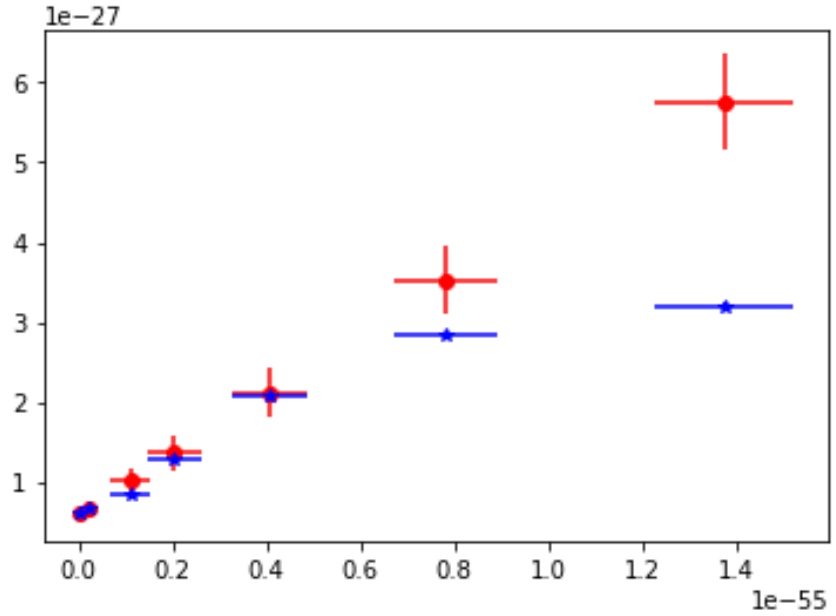

Figure 5: The square of the pulse duration, τ_{FWHM} plotted over the square of the GDD for the measured values and the theoretical calculations.

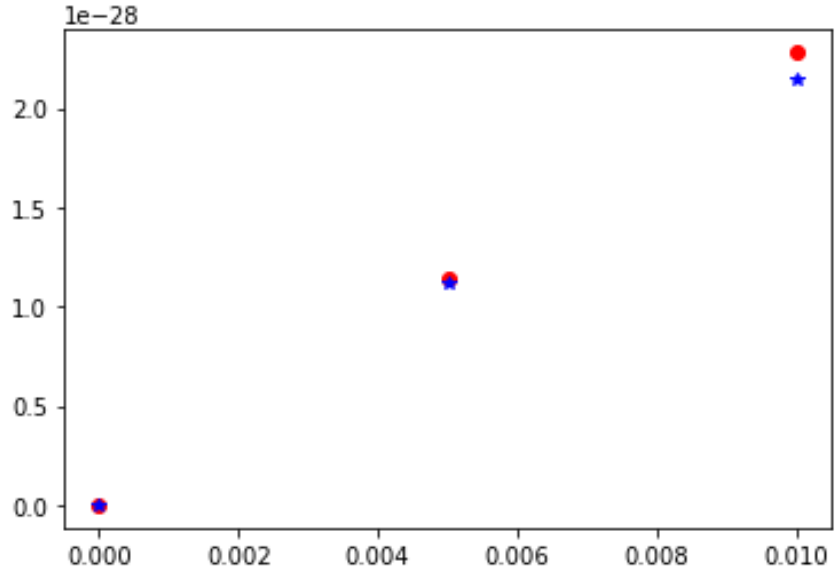

Figure 6: $|GDD|$ over the path length, L_g, of BK7 glass. Shown here is both the theoretical prediction and the required compensation in order to obtain the unchirped pulse.

Material	$\lvert GDD_{theo}\rvert$[fs^2].	$\lvert GDD_{comp}\rvert$[fs^2]	$\tau_{FWHM,meas}$[fs]	$\tau_{FWHM,VChirp}$[fs]
5 mm BK7	114	112	29.6	37.5
10 mm BK7	228	214	51.6	66.7
5 mm MgF2	89	8	24.4	24.7
5 mm BK7 $+30°$	121	120	30.1	39.1
5 mm BK7 $-30°$	121	114	30.6	39.1

Table 1: Expected GDD compared with measured GDD for the various optical elements in this experiment. Also icnluded is the pulse width as measured after inserting the element, $\tau_{FWHM,meas}$, and the pulse width simulated using the software VChirp, $\tau_{FWHM,VChirp}$.

Material	$\lvert GDD_{theo}\rvert$[fs^2].	$\lvert GDD_{comp}\rvert$[fs^2]	$\tau_{FWHM,meas}$[fs]
5 mm BK7	112	108	37.2
10 mm BK7	223	200	49.4

Table 2: Expected GDD compared with measured GDD and the measured pulse width, $\tau_{FWHM,meas}$, using the second bandwidth.

4.3 The Second Bandwidth

For the second bandwidth, we attempted to repeat the first part of the previous section and proceed with evaluating the prism compressor at multiple insertions. Unfortunately during the experiment we falsely assumed that the previous insertion value which produced an unchirped beam would also do so with the new laser configuration. This is undoubtedly not the case and as a result we lack the knowledge of the lasers properties. The carrier frequency appeared noticeable closer to $\lambda_0 = 800,$ nm than before, but the pulse duration and bandwidth remain unknown. Consequently, a quantitative discussion of the results is not possible and we resort to a qualitative summary of the effects of insertion variation and the addition of the two BK7 optical windows.

5 Discussion